Heliyon 10 (2024) e27205

Contents lists available at ScienceDirect

Heliyon

journal homepage: www.cell.com/heliyon

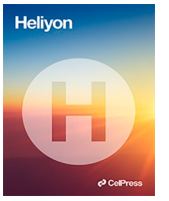

Research article

IDI1 inhibits the cGAS-Sting signaling pathway in hepatocellular carcinoma

Lin Fu *, Hui Ding, Yangqiu Bai **, Lina Cheng, Shanshan Hu, Qiongya Guo

Department of Gastroenterology, Zhengzhou University People's Hospital, Henan Provincial People's Hospital, 7th Weiwu Road, Zhengzhou, 450000, Henan, China

ARTICLE INFO

Keywords:
Hepatocellular carcinoma
IDI1
cGAS
TRIM41

ABSTRACT

Metabolic reprogramming is one of the prominent features that distinguishes tumor cells from normal cells. The role of metabolic abnormalities in regulating innate immunity is poorly understood. In this study, we found that IDI1 is significantly upregulated in liver cancer. IDI1 has no significant effect on the growth or invasion of liver cancer cells but significantly promotes liver cancer development in mice. Through molecular mechanism studies, we found that IDI1 interacts with the important regulator of innate immunity cGAS and recruits the E3 ligase TRIM41 to promote cGAS ubiquitination and degradation, inhibiting the cGAS-Sting signaling pathway. IDI1 inhibits the phosphorylation of TBK1 and the downstream factor IRF3 as well as the expression of CCL5 and CXCL10. In summary, this study revealed the important role of the metabolic enzyme IDI1 in the regulation of innate immunity, suggesting that it may be a potential target for liver cancer treatment.

1. Introduction

Liver cancer is one of the most common malignant tumors. Every year, 700,000 people worldwide die from liver cancer [1]. Currently, clinical treatment methods for liver cancer include multikinase inhibitors (such as sorafenib and lenvatinib) and immune checkpoint inhibitors (such as anti-PD-1 and anti-CTLA4 monoclonal antibodies) [2]. In particular, the application of immune checkpoint inhibitors has greatly improved patient survival [2,3]. However, immunotherapy also has limitations [2–4], and determining approaches to increase the response rate to immunotherapy is an urgent unmet need in clinical tumor treatment.

In the context of tumor immunotherapy, it has been reported that activating the cGAS-STING signaling pathway and creating a proinflammatory immune microenvironment are necessary for the response to anti-PD-1 antibody-mediated immunotherapy in vivo [5,6]. cGAS can sense free DNA in the cytoplasm [7]. The binding of to double-stranded DNA (dsDNA) results in the formation of a cGAS-dsDNA complex, which allows cGAS to synthesize the second messenger cGAMP, thereby activating STING and downstream signaling cascades and promoting the expression of IFN and inflammatory chemokines [7,8].

The regulation of cGAS is a key step in tumor immunotherapy [6]. The cGAS protein can undergo various modifications, such as phosphorylation [9], acetylation [10], ubiquitination [11], and palmitoylation [12]. These modifications can affect the ability of cGAS to bind to DNA or the enzymatic activity of cGAS. In addition, under different physiological and pathological conditions, multiple E3 ligases (such as UBE3C and TRIM14) can regulate the degradation of cGAS through the ubiquitination pathway, thereby modulating

* Corresponding author.
** Corresponding author. Henan Provincial People's Hospital, 7th Weiwu Road, Zhengzhou, 450000, Henan, China.
E-mail addresses: fufu0623@126.com (L. Fu), doctbai@126.com (Y. Bai).

https://doi.org/10.1016/j.heliyon.2024.e27205
Received 5 November 2023; Received in revised form 22 February 2024; Accepted 26 February 2024
Available online 1 March 2024

the activity of the cGAS-Sting signaling axis [13,14]. These studies suggest that the regulation of cGAS can occur at multiple levels.

Metabolic reprogramming is one of the prominent features that distinguishes tumor cells from normal cells. Cholesterol synthesis and metabolism are highly activated in various tumors [15], such as pancreatic and breast tumors [16]. The rate-limiting enzyme in cholesterol synthesis, HMGCR, is upregulated in multiple tumors [16]. IDI1 is responsible for catalyzing the conversion of isopentenyl diphosphate (IPP) into its highly electrophilic isomer dimethylallyl diphosphate (DMAPP) [17]. Deng et al. reported that IDI1 is upregulated in pancreatic cancer and is a target gene of the beta-catenin/TCF signaling pathway [16]. However, the functional role and mechanism of IDI1 in tumors are still not well understood.

In this study, we investigated the expression pattern of IDI1 in liver cancer and explored its function and related mechanisms in the progression of liver cancer.

2. Materials and methods

2.1. Cell culture

Liver cancer cell lines and the normal liver cell line HHL5 were obtained from the Cell Bank of the Chinese Academy of Sciences. The cells were cultured in DMEM. All media were supplemented with 10% fetal bovine serum and double antibiotics (100 U/mL penicillin and 100 μg/mL streptomycin). The cells were cultured in a constant temperature incubator (5% CO_2, 37 °C). Cell transfection was performed using Lipofectamine 8000 according to the product manual.

2.2. Immunohistochemistry

The tissue sections were deparaffinized, rehydrated, and subjected to high-temperature antigen retrieval in EDTA solution for 30 min. After the samples were allowed to cool naturally to room temperature, endogenous peroxidase activity was blocked with an endogenous peroxidase inhibitor for 15 min. The tissue sections were then washed with PBS 1–2 times and incubated overnight at 4 °C with an anti-IDI1 antibody (Abcam, ab97448, 1:300) or anti-ki67 antibody (Proteintech, 27309-1-AP, 1:8000). On the second day, the tissue sections were washed with PBS 3 times and incubated with an appropriate secondary antibody at room temperature for 2 h. Immunohistochemical reactions were visualized using 3,3′-diaminobenzidine (DAB). All tissue sections were counterstained with hematoxylin, and the staining intensity and protein expression levels were automatically scored using the Vectra2 system.

2.3. Western blotting

Cells were washed twice with PBS and then lysed on ice using RIPA lysis buffer containing protease and phosphatase inhibitors. Tissues were cooled with liquid nitrogen, ground, and then lysed on ice using RIPA lysis buffer containing protease and phosphatase inhibitors. After centrifugation, the cell lysate supernatant was collected, and the protein concentration was quantified using a BCA protein assay kit. Equal amounts of protein were separated by SDS−PAGE, transferred to a PVDF membrane, and incubated with specific primary antibodies overnight at 4 °C. After incubation with HRP-conjugated secondary antibodies for 1–2 h, immunoreactivity was detected using a chemiluminescent substrate (Millipore, WBKLS0050) and analyzed using Image Lab software. The primary antibodies used in this experiment included anti-IDI (Abcam, ab97448, 1:1000), anti-tubulin (Santa Cruz Biotechnology, sc-5286, 1:4000), anti-Flag (Proteintech, 66008-4-lG, 1:1000), anti-GAPDH (Proteintech, 10494-1-AP, 1:1000), anti-GST tag (Abcam, ab307273, 1:1000), anti-cGAS (Proteintech, 26416-1-AP, 1:1000), anti-HA (Proteintech, 66006-2-Ig, 1:1000), anti-TRIM41 (Proteintech, 18468-1-AP, 1:1000), anti-*p*-TBK1 (Abcam, ab186469, 1:1000), anti-TBK1 (Proteintech, 28397-1-AP, 1:1000), anti-IRF3 (Proteintech, 66670-1-Ig, 1:1000), and anti-*p*-IRF3 (Abcam, ab76493, 1:1000) antibodies.

2.4. Overexpression and knockdown of IDI1

shRNAs targeting IDI1 and TRIM41 were designed using the Sigma website and were then cloned and inserted into the pLKO.1-puro vector. Lentivirus was packaged in 293T cells with the packaging plasmid psPAX2 and the envelope plasmid pMD2.G. The collected virus was concentrated using PEG8000 and was then centrifuged at 4 °C and 1600×*g* for 1 h. The supernatant was removed, and the pellet was dissolved in 2 ml of DMEM. Cells were seeded at a density equivalent to 50–60% coverage in a 6-well plate. The next day, 400 μl of lentivirus was added to the cells, which were subsequently incubated overnight in a constant-temperature incubator. After two days of lentiviral infection, the cells were cultured with puromycin (1 mg/mL) for 4 days to select for stably transduced cells. The expression of IDI1 and TRIM41 was measured using Western blotting.

2.5. CCK-8 assay

Cells were seeded in a 96-well plate at a density of 1 × 10^3 cells per well and cultured in a constant temperature incubator (37 °C, 5% CO_2). The next day, the old medium was replaced with fresh medium containing 10% CCK-8 reagent, and the plate was incubated in the incubator for 2 h. The absorbance at 450 nm was measured daily beginning one day after the start of the experiment.

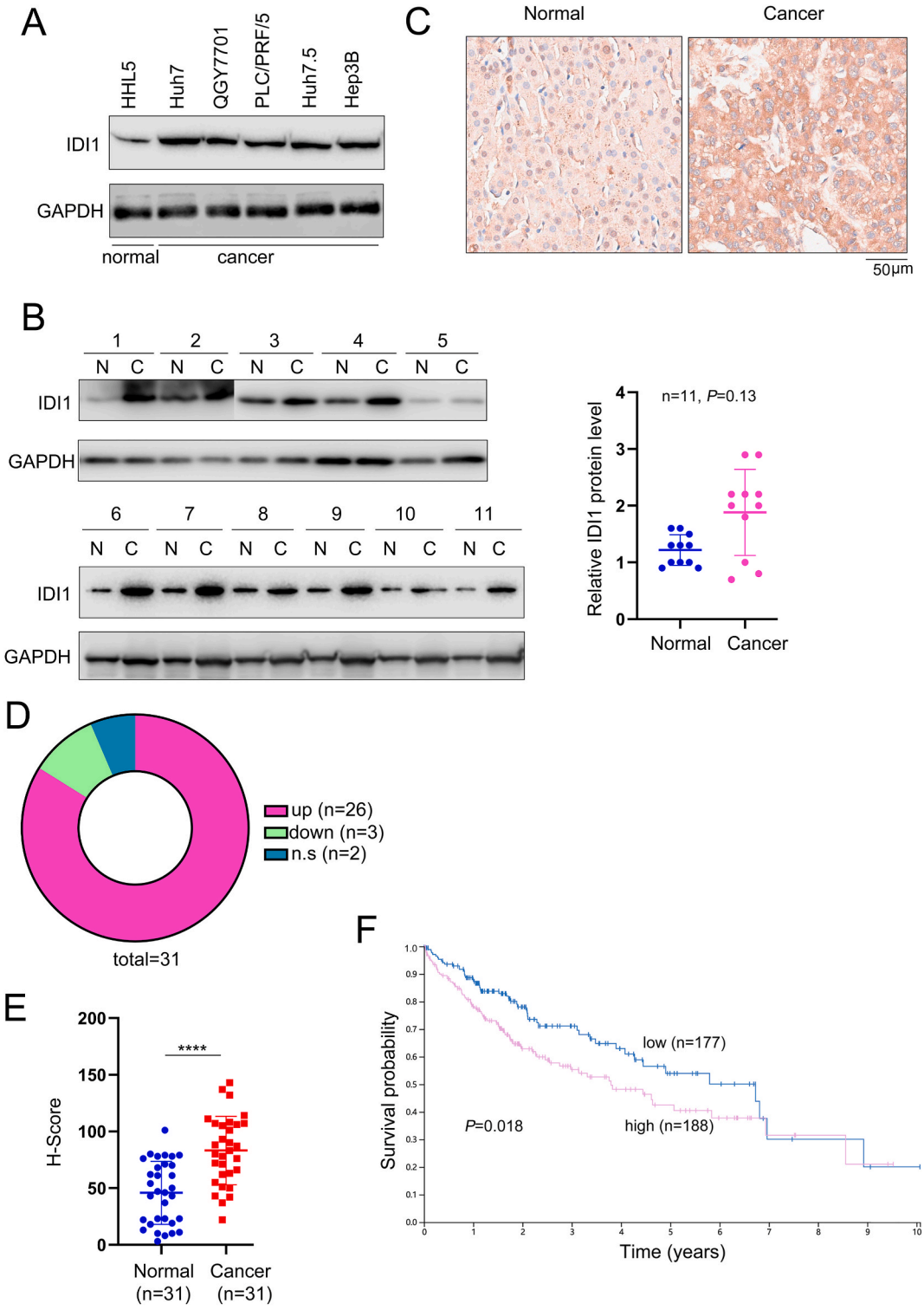

Fig. 1. Upregulation of IDI1 in liver cancer. (A) IDI1 expression in normal liver cells and liver cancer cells, as measured by Western blotting. (B) Protein levels of IDI1 in adjacent tissues (N) and liver cancer tissues (C), as measured by Western blotting; the relative protein levels of IDI1 were analyzed statistically. (C–E) Protein levels of IDI1 in adjacent tissues (Normal) and liver cancer tissues (Cancer), as evaluated by IHC staining; the pie chart was generated and statistical analysis was performed. ****, $P < 0.0001$. Scale bar, 50 μm. (F) Analysis of the relationship between IDI1 expression and the survival of liver cancer patients using the Human Protein Atlas (HPA) database.

2.6. Transwell assay

Sixty-five microliters of Matrigel diluted with basal RPMI-1640 medium (v:v, 100:3) was added to the center of the membrane forming the bottom surface of the upper chamber and incubated at 37 °C for 30 min to allow solidification. The cell suspension was prepared with culture solution containing 0.1% FBS, and the density of the suspension was adjusted to 5×10^5 cells/ml. Then, 200 μL of the cell suspension was seeded in the upper chambers, 500 μL of medium containing 30% FBS was added to the lower chambers of the 24-well plate, and the plate was placed in an incubator at 37 °C with 5% CO_2 for 60 h. After washing three times with PBS, the cells on the bottom surface of each membrane were fixed with 4% paraformaldehyde and stained with 0.3% crystal violet. Five fields of view were randomly selected for observation at 20 × magnification under a microscope (Leica DMI4000B, Germany), and the cells were then imaged and counted with ImageJ software (National Institutes of Health, Bethesda, MD, USA) to calculate the relative invasion rate.

2.7. Hydrodynamic injection

We induced intrahepatic bile duct cancer in C57BL/6 mice via hydrodynamic injection. Plasmids (20 μg of pT3-EF1a-HA-myr-AKT, 30 μg of pT3-EF1a-YapS127A, 20 μg of pT3-EF1a or 20 μg of PT3-EF1a-IDI1) were mixed in 1.5 mL of 0.9% NaCl solution and passed through a 0.22 μm filter membrane for sterilization. Within 5–7 s, 20 μg of the pT3-EF1a-HA-myr-AKT plasmid, 30 μg of the pT3-EF1a-YapS127A plasmid, 20 μg of the control pT3-EF1a plasmid or 20 μg of the PT3-EF1a-IDI1 expression plasmid was injected into the mice via the tail vein. The relevant experiments in this study were approved by the Ethics Committee of Henan Provincial People's Hospital (S2019-084-02).

2.8. Immunoprecipitation

To detect interactions between endogenously expressed proteins, cells were treated and lysed with IP lysis buffer containing proteinase and phosphatase inhibitors. The lysates were centrifuged, and the supernatants were collected. Then, 1 μg of an antibody was added, and the samples were incubated overnight at 4 °C. The next day, 40 μL of Protein A/G beads (bimake.com, B23202) was added, and the samples were incubated at 4 °C for 4 h. The beads were washed three times with wash buffer, after which 1 × loading buffer was added for Western blot analysis.

2.9. GST pull-down assay

Ten micrograms of the GST-cGAS fusion protein was added to cell lysates containing protease and phosphatase inhibitors and incubated overnight at 4 °C. The following day, the Glutathione Sepharose 4B hydrogel beads (GE Healthcare) were washed 3 times with wash buffer (50 mM Tris-HCl (pH 8.0), 150 mM NaCl, and 1% NP-40) and then incubated for 4 additional hours. The beads were washed 3 times with wash buffer (50 mM Tris-HCl (pH 8.0), 150 mM NaCl, and 1% NP-40), 1 × loading buffer was added, and the mixture was heated at 100 °C for 5 min. The supernatant was collected for Western blot analysis.

2.10. qPCR

RNA was extracted using TRIzol (Invitrogen) and then reverse transcribed into cDNA using the PrimeScript™ RT Reagent Kit (Takara) according to the manufacturer's instructions. qPCR was performed using the SYBR Green Reagent Kit and the CFX96 Real-Time PCR Detection System (Bio-Rad, Richmond, CA, USA), with 18S serving as the internal reference. The expression of each target gene was calculated using the $2-\Delta\Delta Ct$ method.

2.11. Statistical analysis

The experimental results are expressed as the mean ± SD values. The data were analyzed using a *t*-test. The Kaplan–Meier method was used to generate survival curves, and the log-rank test was used for analysis. Statistical analysis was performed using GraphPad Prism 8 and SPSS 17.0 software.

3. Results

3.1. IDI1 is upregulated in liver cancer

To further explore the expression pattern of IDI1 in liver cancer, we first examined its expression in liver cancer cell lines (Huh7, QGY7701, PLC/PRF/5, Huh7.5 and Hep3B) and normal liver cells (HHL5). The results showed that IDI1 was upregulated in liver cancer cells (Fig. 1A). Western blot and immunohistochemical analyses of paired liver cancer tissues and adjacent noncancerous tissues also revealed upregulation of IDI1 in liver cancer tissues (Fig. 1B–E). High expression of IDI1 in liver cancer patients, as found in the Human Protein Atlas database (https://www.proteinatlas.org/ENSG00000067064-IDI1/pathology/liver+cancer), suggested a poor prognosis (Fig. 1F). These results suggest that IDI1 plays a crucial role in the progression of liver cancer.

3.2. IDI1 promotes liver tumorigenesis in vivo

To further elucidate the function of IDI1 in the malignant progression of liver cancer, we first overexpressed IDI1 in Huh7 and QGY7701 cells or knocked down IDI1 expression in Huh7 and PLC/PRF/5 cells (Fig. 2A). However, the CCK-8 assays showed that overexpressing IDI1 had no effect on the growth of liver cancer cells (Fig. 2B). Additionally, the Transwell assays showed that knocking down IDI1 did not affect the invasive ability or growth of liver cancer cells (Fig. 2C–E). It has been reported that hepatic overexpression of AKT and YAP in mice can rapidly induce liver cancer. Next, we overexpressed AKT, YAP, and IDI1 in the livers of C57BL/6 mice via hydrodynamic injection. Ectopic expression of IDI1 significantly promoted the occurrence and development of liver cancer (Fig. 2F–G). Additionally, tumors derived from cells with overexpression of IDI1 had a higher proliferation index (Fig. 2H). This finding suggests that IDI1 likely promotes liver cancer progression by affecting the immune microenvironment.

3.3. IDI1 inhibits the cGAS-sting-TBK1 signaling pathway

The innate immune system plays a crucial role in reshaping the tumor immune microenvironment [6]. We first examined the effect of IDI1 on the cGAS-Sting-TBK1 signaling pathway. Overexpression of IDI1 inhibited the phosphorylation of TBK1 (Fig. 3A), while knockdown of IDI1 exhibited cooperative effects with IR exposure or HT-DNA stimulation to increase the phosphorylation of TBK1 and IRF3 (Fig. 3B–D). Consistently, overexpression of IDI1 suppressed the expression of downstream target genes of IRF3 (CXCL10 and CCL5) (Fig. 3E). These results suggest that IDI1 has an inhibitory effect on the cGAS-Sting-TBK1 signaling pathway.

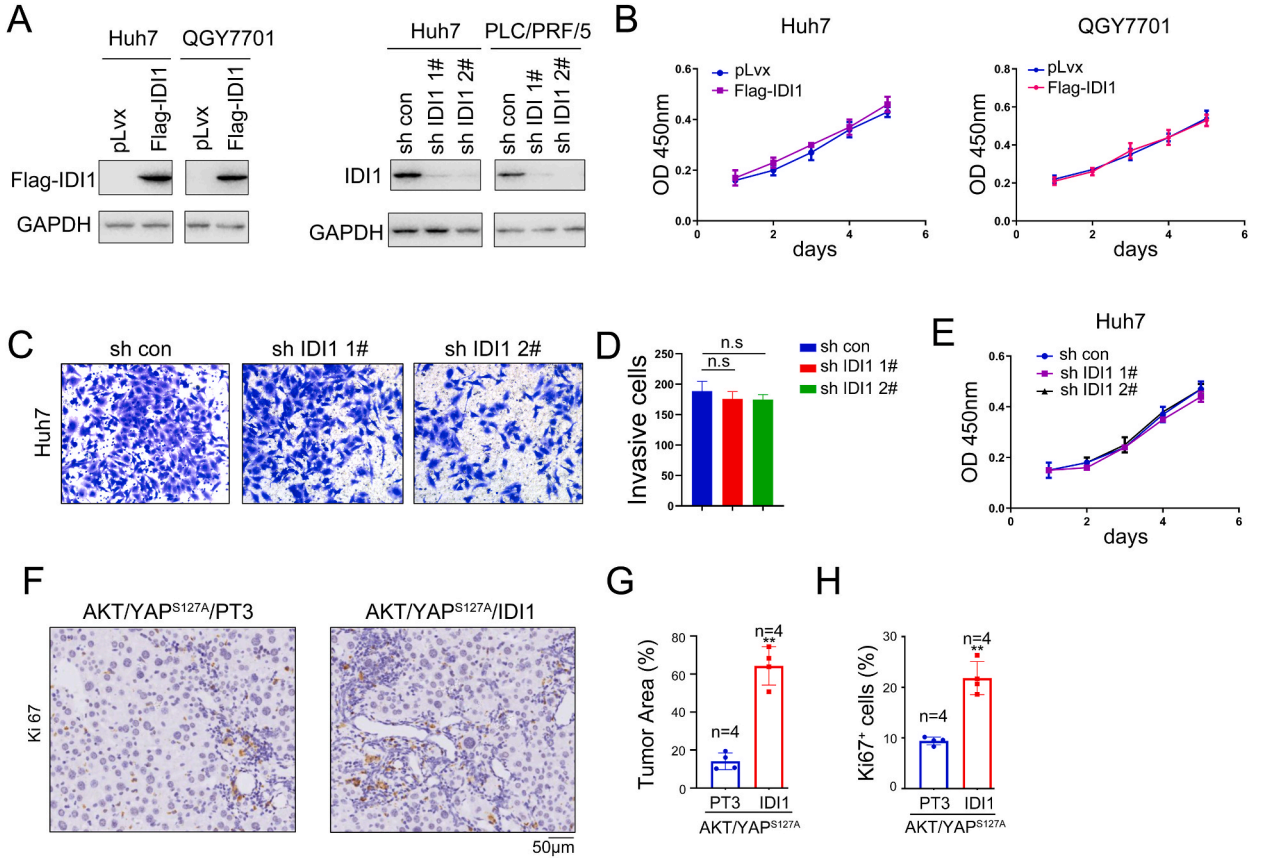

Fig. 2. The expression of IDI1 has no significant impact on the growth or invasion of liver cancer cells but promotes the occurrence of liver cancer in mice. (A) Overexpression of exogenous IDI1 (Flag-IDI1) and knockdown of endogenous IDI1 in liver cancer cells were evaluated by Western blotting. (B) The impact of IDI1 overexpression on the in vitro growth of liver cancer cells was evaluated by a CCK-8 assay. (C–D) The impact of IDI1 knockdown on the invasion of liver cancer cells was evaluated by a Transwell assay. Statistical analysis was performed. (E) The effect of IDI1 knockdown on the in vitro growth of Huh7 cells was evaluated by a CCK-8 assay. (F–H) The impact of IDI1 overexpression in the liver on the occurrence of liver cancer in mice was evaluated using a model established via hydrodynamic injection, and the tumor area percentage and the proportion of Ki67-positive cells were quantified. **, $P < 0.01$.

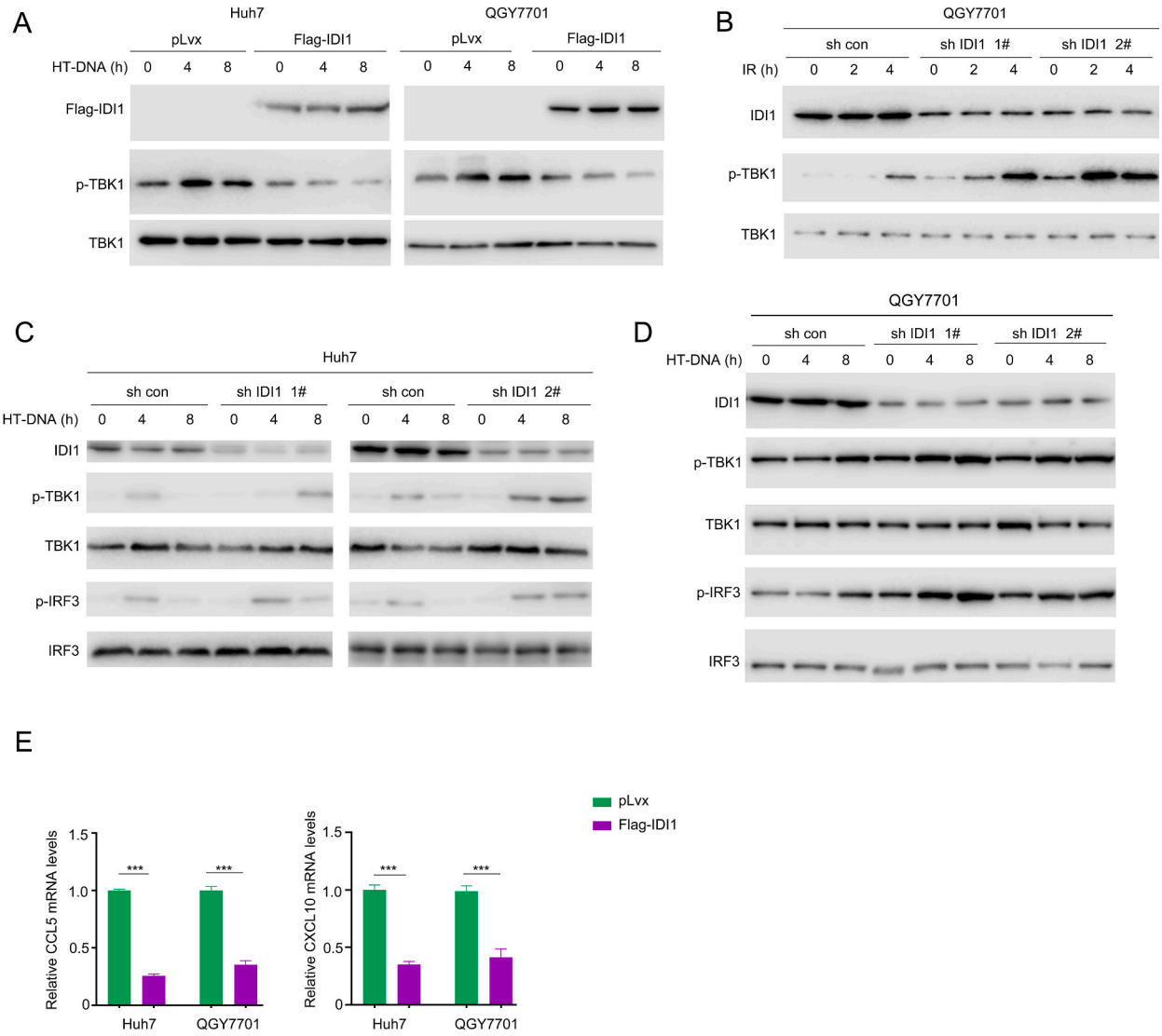

Fig. 3. IDI1 inhibits the cGAS-STING signaling pathway (A) The effect of IDI1 overexpression on the phosphorylation of TBK1 at S172 was evaluated by Western blotting. (B) The effect of IDI1 knockdown on the phosphorylation of TBK1 at S172 upon IR treatment was evaluated by Western blotting. (C–D) The effect of IDI1 knockdown on the phosphorylation of TBK1 (S172) and IRF3 (S386) was evaluated in Huh7 and QGY7701 cells upon stimulation with HT-DNA. (E) The effect of IDI1 overexpression on the expression of CCL5 and CXCL10 was evaluated by qPCR. ***, $P < 0.01$.

3.4. IDI1 interacts with cGAS

Next, we investigated the molecular mechanism by which IDI1 activates the cGAS-Sting-TBK1 signaling pathway from the perspective of protein–protein interactions. We detected the interactions between IDI1 and key components of the cGAS-Sting-TBK1 signaling pathway and found that IDI1 interacts with cGAS (Fig. 4A). In GST pull-down experiments, the fusion protein GST-cGAS was found to bind to endogenously expressed IDI1 (Fig. 4B). Coimmunoprecipitation experiments revealed the interaction between endogenously expressed IDI1 and cGAS (Fig. 4C). Furthermore, after HT-DNA stimulation or IR exposure, the interaction between IDI1 and cGAS was weakened when the cGAS-Sting-TBK1 signaling pathway was activated (Fig. 4D).

To further determine the specific region where IDI1 binds to cGAS, we constructed truncated forms of cGAS containing the N-terminal and C-terminal domains (Fig. 4E). We then performed immunoprecipitation experiments to detect the interactions between IDI1 and these truncated forms. The experimental results indicated that IDI1 binds to the N-terminal domain of cGAS (Fig. 4F).

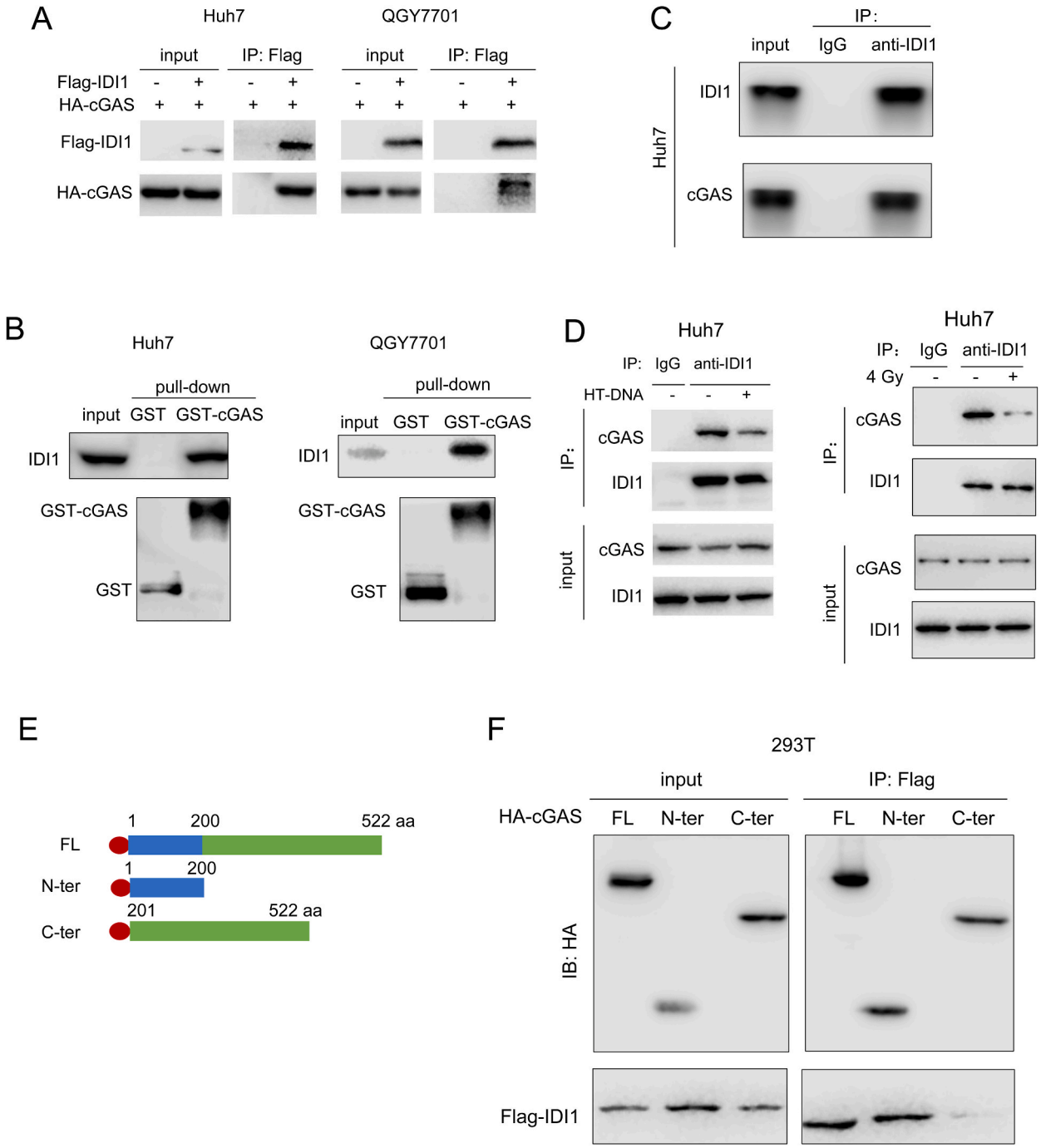

Fig. 4. Interaction between cGAS and IDI1. (A) An immunoprecipitation assay was performed to detect the interaction between exogenously expressed cGAS (HA-cGAS) and IDI1 (Flag-IDI1). (B) A GST pulldown assay was conducted to evaluate the interaction between the GST-cGAS fusion protein and endogenously expressed IDI1 in liver cancer cells. (C) An immunoprecipitation assay was used to investigate the interaction between endogenously expressed cGAS and IDI1 in liver cancer cells. (D) Immunoprecipitation was performed to determine the effect of HT-DNA stimulation or IR (4 Gy) treatment on the interaction between cGAS and IDI1. Cells were transfected with HT-DNA (4 μg) or treated with IR (4 Gy), and after 4 h, the cell lysates were collected and subjected to immunoprecipitation using an anti-IDI1 antibody. (E) Schematic diagram of full-length (FL) cGAS and the cGAS truncations. (F) Immunoprecipitation was used to identify the region in the cGAS protein that is responsible for the interaction between the cGAS protein and IDI1. The N-terminus and C-terminus of cGAS were cloned and cotransfected with Flag-IDI1 into 293T cells. Forty-eight hours later, coimmunoprecipitation was performed.

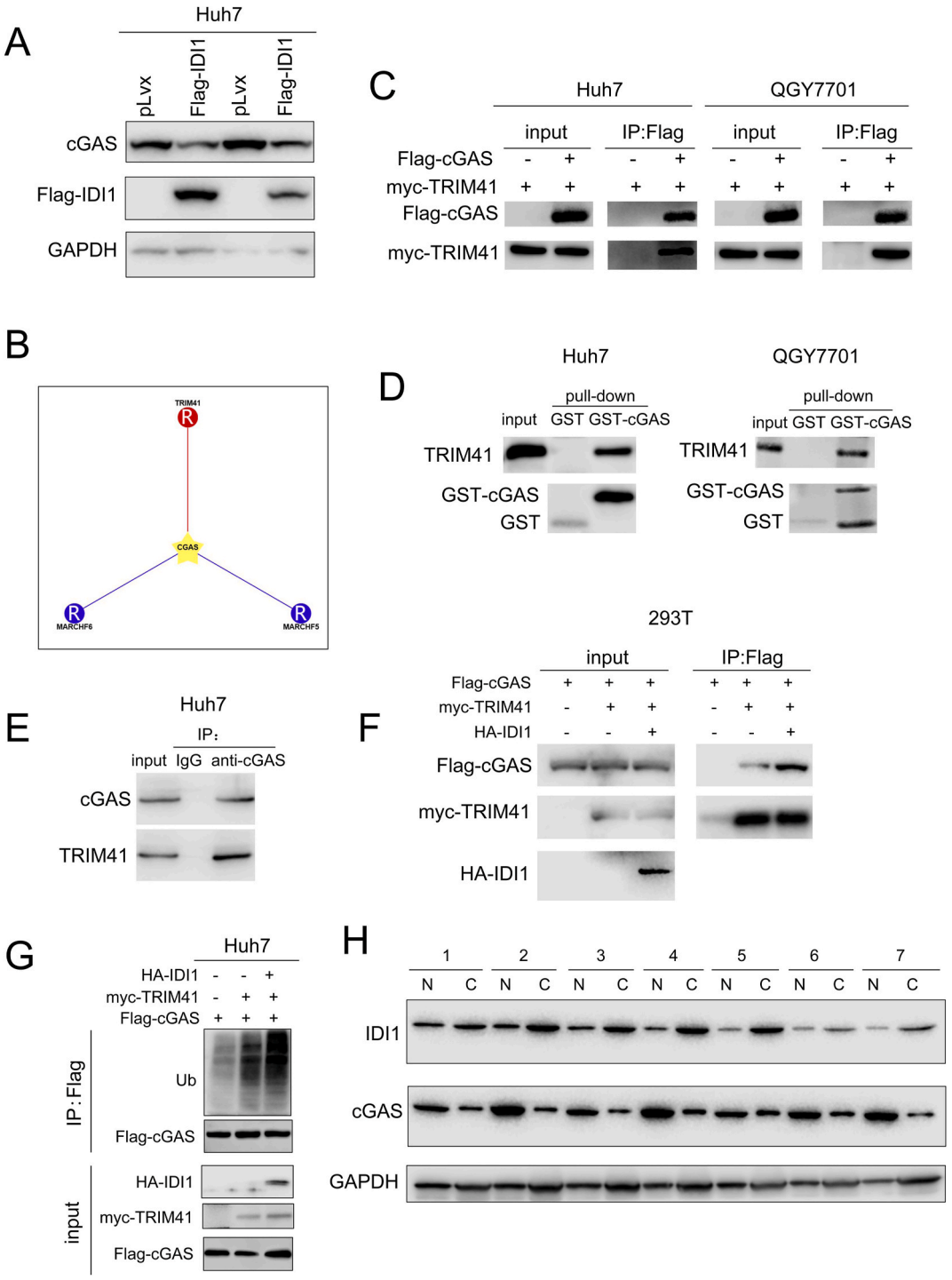

Fig. 5. IDI1 promotes the degradation of cGAS through the ubiquitination pathway. (A) Western blot analysis of the effect of exogenously over-expressed IDI1 (Flag-IDI1) on the level of the endogenous cGAS protein. (B) Prediction of the E3 ligase for cGAS using the UbiBrowser database, revealing TRIM41 as a potential candidate. (C) An immunoprecipitation assay was performed to detect the interaction between exogenously expressed TRIM41 (myc-TRIM41) and cGAS (Flag-cGAS). (D) A GST pull-down experiment was performed to evaluate the interaction between the GST-cGAS fusion protein and endogenously expressed TRIM41 in liver cancer cells. (E) An immunoprecipitation assay with an anti-cGAS antibody was performed to detect the interaction between endogenously expressed cGAS and TRIM41 in liver cancer cells. (F) An immunoprecipitation assay was performed to assess the effect of overexpressed IDI1 (HA-IDI1) on the interaction between exogenously expressed cGAS (Flag-cGAS) and TRIM41 (myc-TRIM41). (G) A ubiquitination assay was performed to investigate the impact of IDI1 expression on the ubiquitination of cGAS. (H) The protein levels of cGAS and IDI1 in HCC clinical samples (C) and adjacent tissues (N) were measured using Western blotting.

3.5. IDI1 promotes cGAS degradation through TRIM41

In further studies, we found that overexpression of IDI1 inhibited cGAS expression (Fig. 5A). Using the UbiBrowser website, we predicted the E3 ligase for cGAS and identified TRIM41 as a potential E3 ligase for cGAS (Fig. 5B). We first confirmed the interaction between TRIM41 and cGAS. In liver cancer cells, exogenously expressed TRIM41 interacted with cGAS (Fig. 5C). In GST pull-down experiments, the fusion protein GST-cGAS was found to bind to endogenously expressed TRIM41 (Fig. 5D). Furthermore, immunoprecipitation experiments showed that endogenously expressed TRIM41 forms a complex with cGAS (Fig. 5E).

Next, we investigated the role of IDI1 in the TRIM41-mediated degradation of cGAS. Overexpression of IDI1 promoted the interaction between cGAS and TRIM41 (Fig. 5F), as well as the ubiquitination of cGAS (Fig. 5G). In addition, in clinical HCC samples, we observed the opposite expression patterns of IDI1 and cGAS (Fig. 5H). These findings suggest that IDI1 inhibits innate immunity by promoting the degradation of cGAS.

4. Discussion

Metabolic reprogramming is a prominent characteristic that distinguishes tumor cells from normal cells. Many metabolic enzymes, such as those involved in glycolysis and serine synthesis, are significantly upregulated in tumor tissues [18]. The mevalonate pathway has been reported to be significantly activated in various tumors, and the rate-limiting enzyme HMGCR has been extensively studied in the context of tumor progression [16,19]. Although Deng et al. reported that IDI1, a key enzyme in the mevalonate pathway, is upregulated in pancreatic cancer, research on the functional role of IDI1 in tumor progression is limited [16]. In this study, we found that IDI1 is upregulated in liver cancer but has little effect on the malignant phenotype of liver cancer cells in vitro. However, in immunocompetent C57 mice, overexpression of IDI1 in the liver significantly promoted liver cancer progression. This finding suggested that IDI1 may be closely related to immune regulation. Through molecular biology experiments, we found that IDI1 interacts with the key molecule of innate immunity, cGAS. By recruiting TRIM41 for the ubiquitination and degradation of cGAS, IDI1 inhibits the expression of CXCL10 and CCL5, thereby suppressing the recruitment of immune cells.

One of the important findings of this study is that IDI1 regulates the cGAS-STING pathway. The proinflammatory effect of the cGAS-STING pathway is believed to enhance tumor immunotherapy sensitivity [20]. Although previous studies have shown that the metabolic state of the body has a significant impact on the effectiveness of tumor immunotherapy [21], there have been very few reports on metabolic enzymes directly involved in immune regulation. This study revealed the regulatory role of IDI1 in cGAS stability, further increasing our understanding of the biological function of IDI1 and supporting the idea that the metabolic state affects immune regulation [21]. The biological function of IDI1 is to catalyze the conversion of isopentenyl diphosphate (IPP) into its highly electrophilic isomer dimethylallyl diphosphate (DMAPP) [22]. However, whether the regulation of cGAS stability by IDI1 depends on the substrate or product of IDI1 is currently unclear and warrants further exploration.

Another important finding of this study is that TRIM41 promotes cGAS degradation. Previous studies have shown that regulation of cGAS can occur at multiple levels [23]. The mRNA expression of cGAS is regulated by multiple microRNAs [24]. The cGAS protein can undergo various modifications, such as phosphorylation, acetylation, and palmitoylation, which can alter the dimerization or DNA binding of the cGAS protein [23]. It has been discovered that UBE3C and TRIM14 can induce the degradation of the cGAS protein [13,14]. This study reveals the role of TRIM41 in cGAS degradation, further improving our understanding of the regulation of cGAS protein stability. Additionally, in the present study, we found that the interaction between IDI1 and cGAS was weakened after activation of the cGAS-Sting pathway by HT-DNA stimulation. It can be speculated that in the resting state, IDI1 inhibits the activity of cGAS, but the negative regulation of IDI1 by cGAS can be relieved by upstream stimuli.

The development of anticancer drugs based on STING pathway activation has attracted the interest of many scientists. In the laboratory, these candidate drugs have shown great promise, but thus far, they have not demonstrated significant anticancer effects in clinical trials [25]. The ineffectiveness of STING agonists in clinical settings may be due to chromosomal instability, which induces sustained activation of the STING pathway and leads to patient desensitization to STING agonists [26].

In summary, this study revealed that the metabolic enzyme IDI1 regulates the stability of cGAS, thereby modulating the regulatory role of cGAS-Sting, and this finding provides a new target for the treatment of liver cancer.

Data availability

The data can be obtained from the authors upon reasonable request.

Declaration

Liver cancer tissues and paired adjacent tissues were obtained from Henan Provincial People's Hospital. All tissue samples were collected with informed consent from the patients for the study of IDI1 expression in liver cancer tissues. The relevant experiments in this study were approved by the Ethics Committee of Henan Provincial People's Hospital (S2019-084-01).

CRediT authorship contribution statement

Lin Fu: Writing – review & editing, Writing – original draft, Investigation, Formal analysis. **Hui Ding:** Methodology, Investigation. **Yangqiu Bai:** Writing – review & editing, Writing – original draft, Conceptualization. **Lina Cheng:** Formal analysis. **Shanshan Hu:**

Investigation, Formal analysis. **Qiongya Guo:** Formal analysis, Data curation.

Declaration of competing interest

The authors declare that they have no known competing financial interests or personal relationships that could have appeared to influence the work reported in this paper.

Appendix A. Supplementary data

Supplementary data to this article can be found online at https://doi.org/10.1016/j.heliyon.2024.e27205.

References

[1] R.L. Siegel, K.D. Miller, N.S. Wagle, A. Jemal, Cancer statistics, 2023, Ca - Cancer J. Clin. 73 (2023) 17–48.
[2] J.M. Llovet, F. Castet, M. Heikenwalder, M.K. Maini, V. Mazzaferro, D.J. Pinato, E. Pikarsky, A.X. Zhu, R.S. Finn, Immunotherapies for hepatocellular carcinoma, Nat. Rev. Clin. Oncol. 19 (2022) 151–172.
[3] B. Sangro, P. Sarobe, S. Hervás-Stubbs, I. Melero, Advances in immunotherapy for hepatocellular carcinoma, Nature reviews, Gastroenterol. Hepatol. 18 (2021) 525–543.
[4] A.A. Khan, Z.K. Liu, X. Xu, Recent advances in immunotherapy for hepatocellular carcinoma, Hepatobiliary & pancreatic diseases international, HBPD INT 20 (2021) 511–520.
[5] S. Zhou, F. Cheng, Y. Zhang, T. Su, G. Zhu, Engineering and delivery of cGAS-STING immunomodulators for the immunotherapy of cancer and autoimmune diseases, Acc. Chem. Res. 56 (2023) 2933–2943.
[6] Y. Wang, J. Luo, A. Alu, X. Han, Y. Wei, X. Wei, cGAS-STING pathway in cancer biotherapy, Mol. Cancer 19 (2020) 136.
[7] A. Decout, J.D. Katz, S. Venkatraman, A. Ablasser, The cGAS-STING pathway as a therapeutic target in inflammatory diseases, Nat. Rev. Immunol. 21 (2021) 548–569.
[8] K.P. Hopfner, V. Hornung, Molecular mechanisms and cellular functions of cGAS-STING signalling, Nat. Rev. Mol. Cell Biol. 21 (2020) 501–521.
[9] T. Li, T. Huang, M. Du, X. Chen, F. Du, J. Ren, Z.J. Chen, Phosphorylation and Chromatin Tethering Prevent cGAS Activation during Mitosis, Science, New York, N.Y., 2021, p. 371.
[10] J. Dai, Y.J. Huang, X. He, M. Zhao, X. Wang, Z.S. Liu, W. Xue, H. Cai, X.Y. Zhan, S.Y. Huang, K. He, H. Wang, N. Wang, Z. Sang, T. Li, Q.Y. Han, J. Mao, X. Diao, N. Song, Y. Chen, W.H. Li, J.H. Man, A.L. Li, T. Zhou, Z.G. Liu, X.M. Zhang, T. Li, Acetylation blocks cGAS activity and inhibits self-DNA-induced autoimmunity, Cell 176 (2019) 1447–1460.e1414.
[11] X. Yang, C. Shi, H. Li, S. Shen, C. Su, H. Yin, MARCH8 attenuates cGAS-mediated innate immune responses through ubiquitylation, Sci. Signal. 15 (2022) eabk3067.
[12] C. Shi, X. Yang, Y. Liu, H. Li, H. Chu, G. Li, H. Yin, ZDHHC18 negatively regulates cGAS-mediated innate immunity through palmitoylation, EMBO J. 41 (2022) e109272.
[13] Z. Ma, J. Bai, C. Jiang, H. Zhu, D. Liu, M. Pan, X. Wang, J. Pi, P. Jiang, X. Liu, Tegument protein UL21 of alpha-herpesvirus inhibits the innate immunity by triggering CGAS degradation through TOLLIP-mediated selective autophagy, Autophagy 19 (2023) 1512–1532.
[14] M. Chen, Q. Meng, Y. Qin, P. Liang, P. Tan, L. He, Y. Zhou, Y. Chen, J. Huang, R.F. Wang, J. Cui, TRIM14 inhibits cGAS degradation mediated by selective autophagy receptor p62 to promote innate immune responses, Mol. Cell 64 (2016) 105–119.
[15] N.K. Chua, H.W. Coates, A.J. Brown, Cholesterol, cancer, and rebooting a treatment for athlete's foot, Sci. Transl. Med. 10 (2018).
[16] Y.Z. Deng, Z. Cai, S. Shi, H. Jiang, Y.R. Shang, N. Ma, J.J. Wang, D.X. Guan, T.W. Chen, Y.F. Rong, Z.Y. Qian, E.B. Zhang, D. Feng, Q.L. Zhou, Y.N. Du, D.P. Liu, X.X. Huang, L.M. Liu, E. Chin, D.S. Li, X.F. Wang, X.L. Zhang, D. Xie, Cilia loss sensitizes cells to transformation by activating the mevalonate pathway, J. Exp. Med. 215 (2018) 177–195.
[17] P.E. Lázaro-Mixteco, J.M. González-Coronel, L. Hernández-Padilla, L. Martínez-Alcantar, E. Martínez-Carranza, J.S. López-Bucio, A. Guevara-García Á, J. Campos-García, Transcriptomics reveals the mevalonate and cholesterol pathways blocking as part of the bacterial cyclodipeptides cytotoxic effects in HeLa cells of human cervix adenocarcinoma, Front. Oncol. 12 (2022) 790537.
[18] N.N. Pavlova, J. Zhu, C.B. Thompson, The hallmarks of cancer metabolism: still emerging, Cell Metabol. 34 (2022) 355–377.
[19] J.W. Clendening, A. Pandyra, P.C. Boutros, S. El Ghamrasni, F. Khosravi, G.A. Trentin, A. Martirosyan, A. Hakem, R. Hakem, I. Jurisica, L.Z. Penn, Dysregulation of the mevalonate pathway promotes transformation, Proc. Natl. Acad. Sci. U. S. A 107 (2010) 15051–15056.
[20] M. Jiang, P. Chen, L. Wang, W. Li, B. Chen, Y. Liu, H. Wang, S. Zhao, L. Ye, Y. He, C. Zhou, cGAS-STING, an important pathway in cancer immunotherapy, J. Hematol. Oncol. 13 (2020) 81.
[21] J.E. Bader, K. Voss, J.C. Rathmell, Targeting metabolism to improve the tumor microenvironment for cancer immunotherapy, Mol. Cell 78 (2020) 1019–1033.
[22] Y. Zhang, X. Cao, J. Wang, F. Tang, Enhancement of linalool production in Saccharomyces cerevisiae by utilizing isopentenol utilization pathway, Microb. Cell Factories 21 (2022) 212.
[23] B. Song, T.M. Greco, K.K. Lum, C.E. Taber, I.M. Cristea, The DNA sensor cGAS is decorated by acetylation and phosphorylation modifications in the context of immune signaling, Mol. Cell. Proteomics : MCP 19 (2020) 1193–1208.
[24] Q. Yu, L. Chu, Y. Li, Q. Wang, J. Zhu, C. Wang, S. Cui, miR-23a/b suppress cGAS-mediated innate and autoimmunity, Cell. Mol. Immunol. 18 (2021) 1235–1248.
[25] A. Amouzegar, M. Chelvanambi, J.N. Filderman, W.J. Storkus, J.J. Luke, STING agonists as cancer therapeutics, Cancers 13 (2021).
[26] J. Li, M.J. Hubisz, E.M. Earlie, M.A. Duran, C. Hong, A.A. Varela, E. Lettera, M. Deyell, B. Tavora, J.J. Havel, S.M. Phyu, A.D. Amin, K. Budre, E. Kamiya, J. A. Cavallo, C. Garris, S. Powell, J.S. Reis-Filho, H. Wen, S. Bettigole, A.J. Khan, B. Izar, E.E. Parkes, A.M. Laughney, S.F. Bakhoum, Non-cell-autonomous cancer progression from chromosomal instability, Nature 620 (2023) 1080–1088.